

This content has been downloaded from IOPscience. Please scroll down to see the full text.

Download details:

IP Address: 84.17.59.57

This content was downloaded on 16/07/2022 at 13:28

Please note that [terms and conditions apply](#).

You may also like:

[Advances in Modern Sensors](#)

[Simultaneous implementation of various RF passives using a novel RF MEMS process module and metallized air cavity](#)

Sang-Seok Lee, Yukihiya Yoshida, Tamotsu Nishino et al.

[Fabrication of thick silicon nitride blocks embedded in low-resistivity silicon substrates for radio frequency applications](#)

L J Fernández, E Berenschot, R J Wiegerink et al.

[RF-MEMS for future mobile applications: experimental verification of a reconfigurable 8-bit power attenuator up to 110 GHz](#)

J Iannacci and C Tschoban

[10 GHz RF Passive Components Obtained by MCM-D Technology](#)

L. B. Zoccal, C. M. Cabreira, S. D. Yamamoto et al.

RF-MEMS Technology for High-Performance Passives
(Second Edition)

5G applications and prospects for 6G

Jacopo Iannacci

Appendix A

Moving MEMS: Dynamics down in the micro-world

A.1 Introduction

The aim of this appendix is to provide a brief insight into Micro-ElectroMechanical Systems (MEMS) and Radio Frequency Micro-ElectroMechanical Systems (RF-MEMS) dynamics, by reporting and explaining a few video animations of micro-system devices recorded during their operation. The material will be based both on experimental measurements as well as Finite Element Method (FEM) simulations. The way sections are split is based upon the type of measurement setup or simulation exploited to obtain visual dynamic data. According to this arrangement, the necessary background on the observation procedure is provided first, in such a way as to ease understanding.

A.2 Measurements based on interferometric microscopy

The experimental material that is going to be reported in this section is acquired by means of a setup based on optical interferometry. This particular type of microscopy analysis exploits the constructive/destructive interference of the light coming back from the Device Under Test (DUT) with that reflected by a mirror, in order to reconstruct information about the vertical dimension of the DUT itself [1, 2]. In other words, optical interferometry allows one to reconstruct a 3D profile of the DUT, starting from single microscopy observation. Proper software-based post-processing of the measured data enables 3D images rendering of the DUT, in which a colour scale is typically used to provide information about the elevation along the vertical direction of each measured spot. The image reported in figure A.1 shows the 3D topology of an RF-MEMS two-state capacitor obtained with an optical interferometer based on white light. The DUT is a typical MEMS suspended electrostatically controlled plate, framed within a Coplanar Waveguide (CPW) structure.

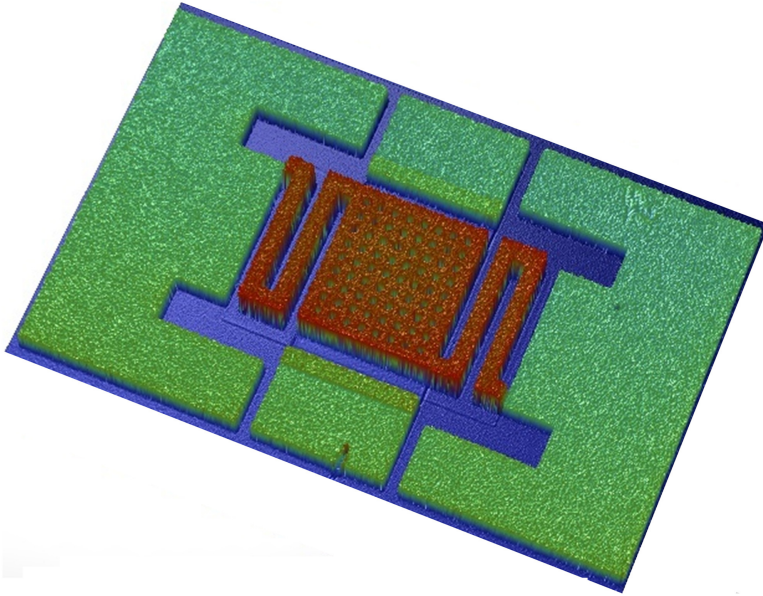


Figure A.1. 3D image of an RF-MEMS two-state capacitor obtained by means of optical interferometry. The colour scale indicates the vertical quote of the DUT.

Looking at the colour scale of the image in figure A.1, three main reference quotes can easily be identified. The lower plane, depicted in blue, is the underlying substrate. The intermediate quote, reported in green, is that of the electrodeposited gold defining the CPW line and ground planes. Finally, the higher level, shown in red, is the elevated MEMS membrane. The central suspended plate with holes and the meandered suspensions are clearly visible. Any additional information about the technology is available in figure 4.2 and table 4.1.

Besides white-light static 3D profiling, interferometric microscopy also enables measurements in dynamic conditions. In this case, the DUT is illuminated with stroboscopic (pulsed) light. This type of measurement can be effectively exploited just to observe periodic behavioural characteristics. The DUT is stimulated by a periodic waveform (e.g. sine, pulse, etc) at a certain frequency. On the other hand, the stroboscopic light is pulsed at the same frequency. The phase delay of the pulse feeding the light source with respect to the bias driving the DUT is increased, period after period. This way, at each iteration of the periodic behaviour, an image of the DUT at a different point of its characteristic is acquired. Finally, by putting together all the collected snapshots, the behaviour of the observed sample over an entire period is reconstructed [3–6].

The RF-MEMS sample in figure A.1 is biased with a zero mean value triangular waveform ranging between -20 V and $+20$ V. The absolute peak value is selected in order to be larger than the pull-in voltage. Moreover, its frequency is kept low (0.05 Hz) in order to perform the measurement in quasi-static conditions. The bias waveform versus time, with markers in the corresponding pull-in and pull-out transitions, is reported in figure A.2.

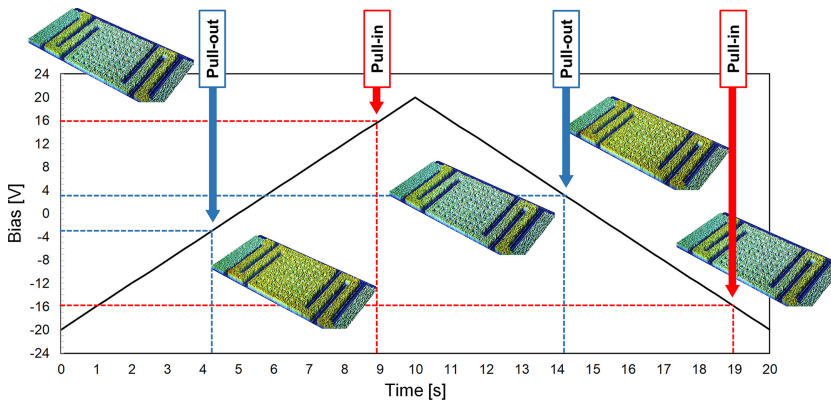
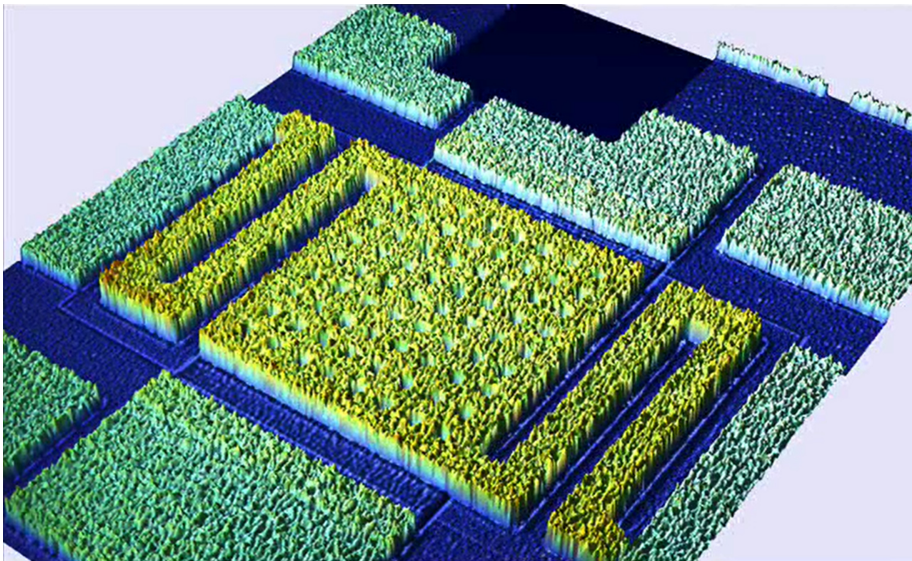


Figure A.2. Triangular waveform versus time biasing the DUT. Pull-in and pull-out levels are indicated along with measured images of the RF-MEMS when actuated (membrane colour closer to green) and not actuated (membrane colour closer to red).



Video A.1. Video animation of the RF-MEMS in figure A.1 when biased by the waveform in figure A.2, as reconstructed by 3D stroboscopic light optical dynamic interferometry. Video available at <https://iopscience.iop.org/book/978-0-7503-4199-8>.

Pull-in takes place at ± 16 V, while pull-out happens at ± 3 V. With the waveform centred around zero, two actuations and releases are observed over one period. The small measured snapshots of the RF-MEMS movable membrane help one to understand what it looks like (in terms of colours) when actuated and not actuated. Finally, an animation of the RF-MEMS, as reconstructed by the 3D stroboscopic light optical interferometric systems, is reported in video A.1.

A dynamic characterisation performed on a different DUT by means of the same measurement procedure discussed above is now going to be reported. The observed RF-MEMS device is a multi-state power attenuator comprising six cantilevered ohmic switches, exploited to select or short resistive loads on a split RF line [7, 8]. The 3D topology of the physical sample, obtained by means of white-light interferometry, is shown in figure A.3.

The DUT is stimulated with a waveform similar to that previously discussed in figure A.2. Transitions of cantilevered switches, corresponding to pull-in and pull-out, are visible in the animation, reconstructed by the 3D stroboscopic light optical interferometric systems, in video A.2.

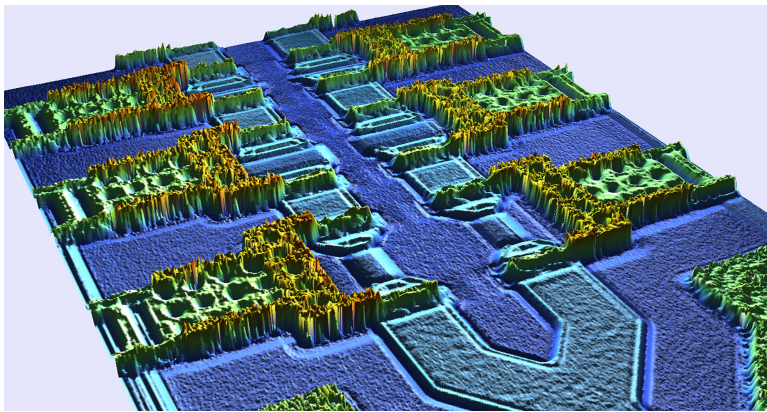
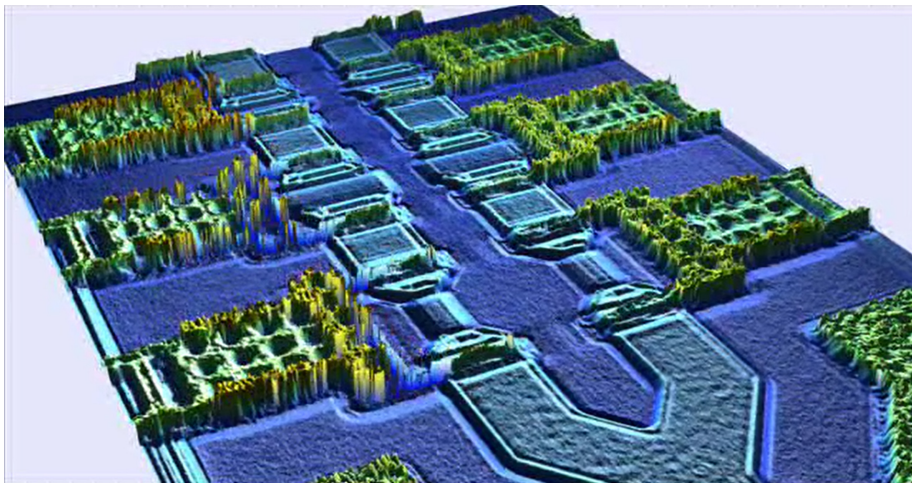


Figure A.3. 3D image of the RF-MEMS power attenuator discussed in [7, 8], obtained by means of optical interferometry. The colour scale indicates the vertical quote of the DUT.



Video A.2. Video animation of the RF-MEMS attenuator in figure A.3 when biased by a waveform similar to that in figure A.2, as reconstructed by 3D stroboscopic light optical dynamic interferometry. Video available at <https://iopscience.iop.org/book/978-0-7503-4199-8>.

A.3 Measurements based on laser Doppler vibrometer (LDV) microscopy

In this section a different measurement technique, able to capture the dynamic characteristics of RF-MEMS, is exploited. It is called Laser Doppler Vibrometer (LDV) microscopy, and exploits the Doppler effect in order to reconstruct the movement of a certain spot pointed by a laser light source, i.e. if getting closer or farther with respect to the source [9–11]. Differing from dynamic interferometry, LDV microscopy enables one to capture the real-time evolution of the DUT. In other words, there is no need to cycle the sample many times to build its dynamics over one period. Nonetheless, the laser spot monitors just one point over the DUT surface. Therefore, if one wants to observe the dynamic characteristic of a certain sample portion, the biasing waveform has to be cycled several times, in order for the laser to acquire a different spot, period after period, and then reconstruct the evolution of a surface rather than of a single point.

The DUT example selected for LDV microscopy investigation is an RF-MEMS toggle-type switch. This particular geometry employs two suspended electrostatic actuators, anchored in their central point. Each actuator is provided with two distinct counter-electrodes for DC/AC biasing. Depending on whether the inner or outer electrodes are driven (pull-down and pull-up, respectively), the central plate can be displaced downwards or upwards, thus extending the vertical range it can span [12–14]. The layout of the RF-MEMS toggle switch exploited for LDV microscopy dynamic measurement is shown in figure A.4.

In the experimental setup, the pull-down and pull-up electrodes are alternately biased, so that the actuators can tilt both clockwise and counter clockwise around the axis passing through flexible suspensions and anchoring points. The dynamic response captured by means of LDV microscopy is reported in video A.3. In the animation, the surface measured with the laser source (i.e. the moving one) is reported in colours, and the colour scale indicates the vertical displacement extent. Such a surface is superimposed on the grayscale measurement of the DUT. Since the entire RF-MEMS toggle switch is larger than the maximum surface observable with the experimental setup, it was not possible to display the whole structure in the animation.

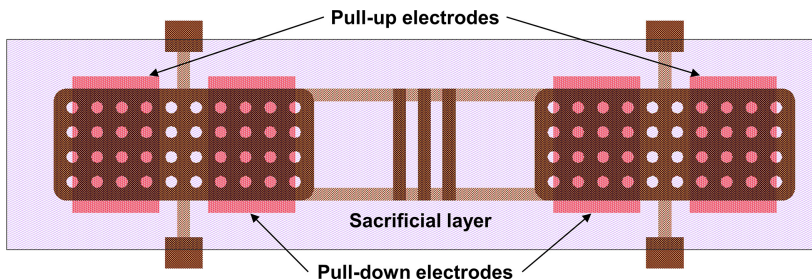
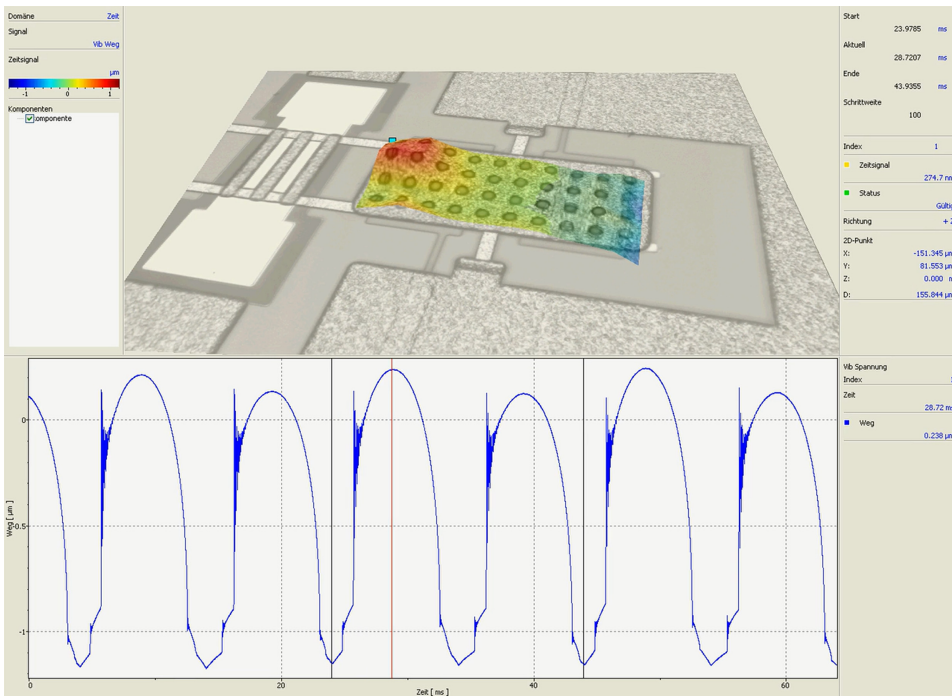


Figure A.4. Layout of the RF-MEMS toggle switch exploited for dynamic characterisation based on LDV microscopy.



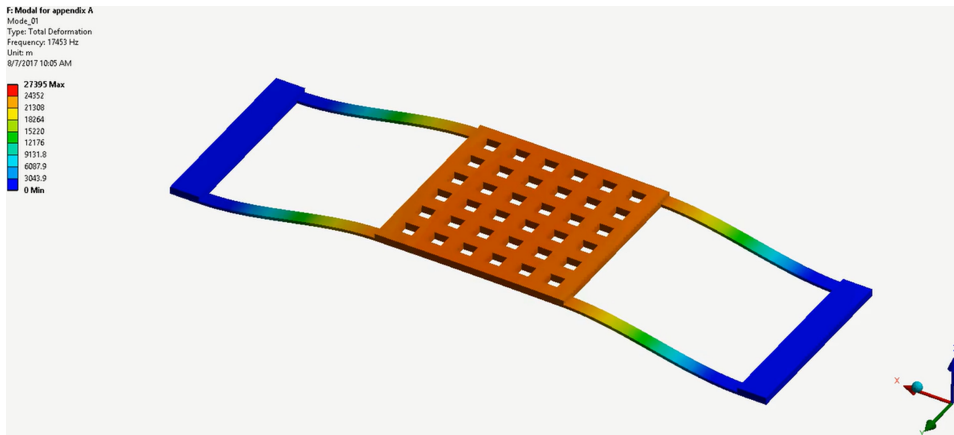
Video A.3. Video animation of the RF-MEMS toggle-switch in figure A.4 when pull-down and pull-up electrodes are alternately biased, as reconstructed by LDV microscopy dynamic measurement. Video available at <https://iopscience.iop.org/book/978-0-7503-4199-8>.

A.4 Simulated animations

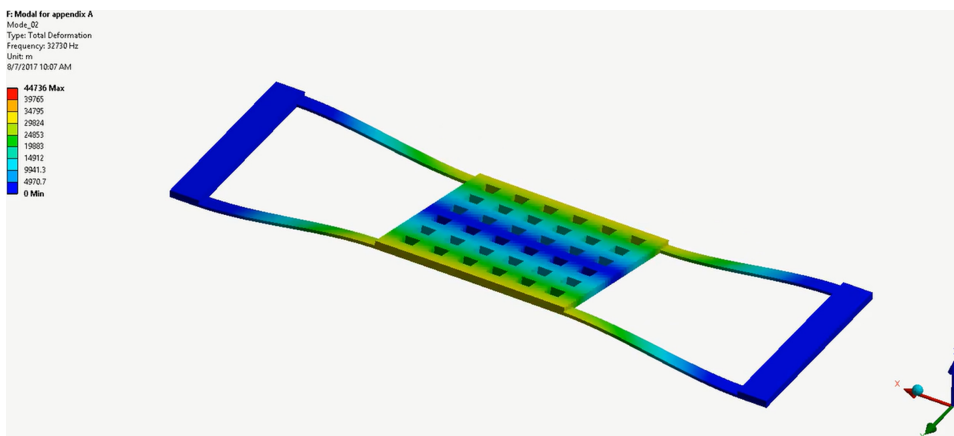
In this section, simulated animations of an RF-MEMS switch are briefly reported. The DUT is the series ohmic micro-relay already discussed in chapter 4 and reported in figures 4.3 and 4.5. Simulations are performed in Ansys Workbench, and the type of analysis is modal eigenfrequency, previously mentioned in section 4.3.2. The predicted resonant modes, from the fundamental (first mode) to the fourth one, are reported in the animations in video A.4, video A.5, video A.6 and video A.7, respectively.

A.5 Conclusion

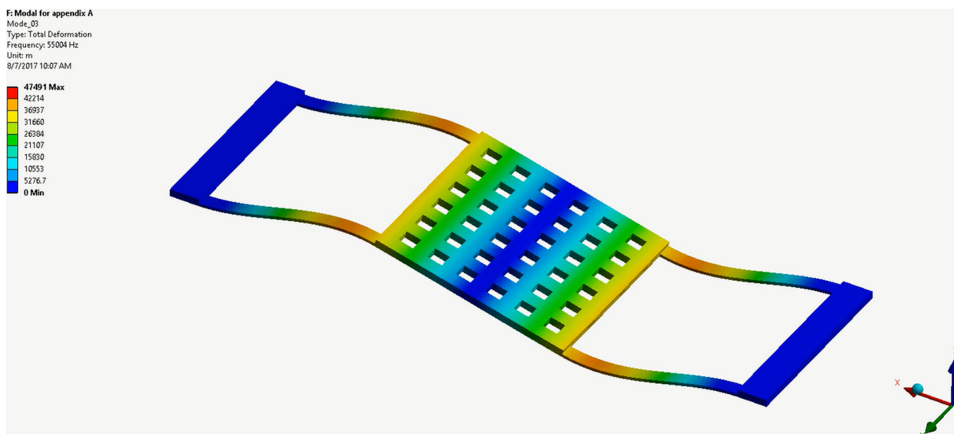
In this appendix, a few significant examples of moving MEMS were reported. The reviewed data come both from experimental measurements of physical samples, as well as from Finite Element Method (FEM) simulations. Before showing any Devices Under Test (DUTs) animated dynamics, the specific measurement/simulation procedure was described, in order to ease understanding of the presented material. The content of this appendix complements the overall discussion developed in the previous chapters of this work.



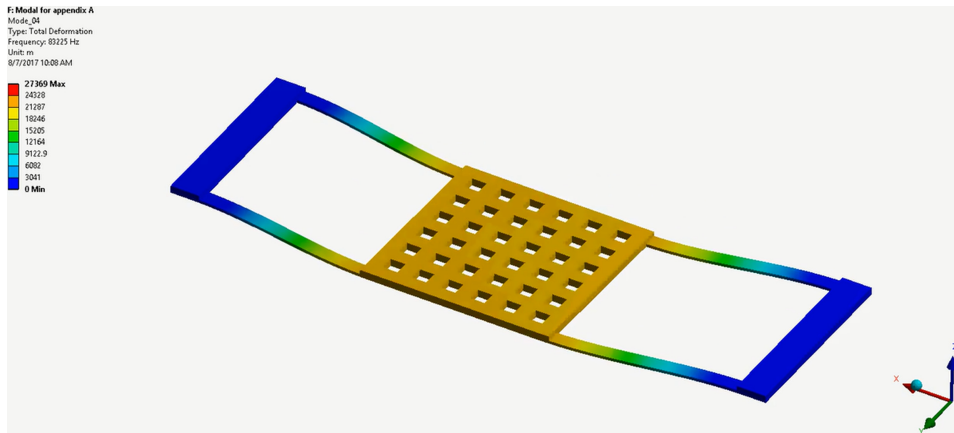
Video A.4. Fundamental resonant mode (1st mode) of the RF-MEMS ohmic switch in figure 4.5. Resonance is predicted by Workbench at 17.4 kHz. Video available at <https://iopscience.iop.org/book/978-0-7503-4199-8>.



Video A.5. 2nd resonant mode of the RF-MEMS ohmic switch in figure 4.5. Resonance is predicted by Workbench at 32.7 kHz. Video available at <https://iopscience.iop.org/book/978-0-7503-4199-8>.



Video A.6. 3rd resonant mode of the RF-MEMS ohmic switch in figure 4.5. Resonance is predicted by Workbench at 55 kHz. Video available at <https://iopscience.iop.org/book/978-0-7503-4199-8>.



Video A.7. 4th resonant mode of the RF-MEMS ohmic switch in [figure 4.5](#). Resonance is predicted by Workbench at 83.2 kHz. Video available at <https://iopscience.iop.org/book/978-0-7503-4199-8>.

References

- [1] Wang S H, Quan C, Tay C J, Reading I and Fang Z P 2003 Deformation measurement of MEMS components using optical interferometry *Meas. Sci. Technol.* **14** 909–15
- [2] Blackshire J L and Sathish S 2002 Characterization of MEMS transducer performance using near-field scanning interferometry *IEEE Trans. Ultrason. Ferroelectr. Freq. Control* **49** 669–74
- [3] Kim B, Razavi H A, Degertekin F L and Kurfess T R 2002 Micromachined interferometer for measuring dynamic response of microstructures *Proc. ASME Int. Mech. Eng. Congress and Exposition, MEMS Symp. (New Orleans, LA, Nov. 2002)*
- [4] Graebner J E 2000 Optical scanning interferometer for dynamic imaging of high-frequency surface motion *Proc. IEEE Ultrasonics Symp. (San Juan, Oct. 2000)* pp 733–6
- [5] Bosseboeuf A and Petitgrand S 2003 Characterization of the static and dynamic behaviour of M(O)EMS by optical techniques: Status and trends *J. Micromech. Microeng.* **13** 23–33
- [6] Chen L-C, Huang Y-T and Chang P-B 2006 High-bandwidth dynamic full-field profilometry for nano-scale characterization of MEMS *J. Phys. Conf. Ser.* **48** 1058–62
- [7] Iannacci J, Faes A, Mastri F, Masotti D and Rizzoli V 2010 A MEMS-based wide-band multi-state power attenuator for radio frequency and microwave applications *Proc. of TechConnect World, NSTI-Nanotech (Anaheim, CA, June 2010)* pp 328–31
- [8] Iannacci J, Faes A, Kuenzig T, Niessner M and Wachutka G 2011 Electromechanical and electromagnetic simulation of RF-MEMS complex networks based on compact modeling approach *Proc. of TechConnect World, NSTI Nanotech 2011 (Boston, MA, June 2011)* pp 591–94
- [9] Lawrence E *Optical Measurement Techniques for Dynamic Characterization of MEMS Devices* http://polytec.com/fileadmin/user_uploads/Applications/Micro_Nano_Technology/Documents/OM_TP_MEMS_Whitepaper_2012_07_E.pdf
- [10] Kim M G, Jo K, Kwon H S, Jang W, Park Y and Lee J H 2009 Fiber-optic laser Doppler vibrometer to dynamically measure MEMS actuator with in-plane motion *IEEE J. Microelectromech. Syst.* **18** 1365–70

- [11] Liu J-W, Huang Q-A, Song J and Tang J-Y 2008 Detection of stiction of suspending structures in MEMS by a laser Doppler vibrometer systems *Proc. Int. Conf. on Solid-State and Integrated-Circuit Technology (Beijing, Oct. 2008)* pp 2472–5
- [12] Schauwecker B, Strohm K A, Simon W, Mehner J and Luy J F 2002 Toggle-switch—a new type of RF MEMS switch for power applications *Proc. IEEE MTT-S Int. Microw. Symp. Digest (Seattle, WA, June 2002)* pp 219–22
- [13] Solazzi F, Tazzoli A, Farinelli P, Faes A, Mulloni V, Meneghesso G and Margesin B 2010 Active recovering mechanism for high performance RF MEMS redundancy switches *Proc. Europ. Microw. Conf. (Paris, Sept. 2010)* pp 93–6
- [14] Schauwecker B, Strohm K M, Mack T, Simon W and Luy J F 2003 Single-pole-double-throw switch based on toggle switch *IET Electron. Lett.* **39** 668–70

RF-MEMS Technology for High-Performance Passives
(Second Edition)

5G applications and prospects for 6G

Jacopo Iannacci

Appendix B

How to set up, configure and exploit the MEMS behavioural models software library

B.1 Introduction

The target of this appendix is that of gathering all the necessary information to set up and exploit the Micro-ElectroMechanical Systems (MEMS) compact model library discussed in the previous chapter 5, according to a user-guide arrangement. The software library is made available for download together with this book, and is implemented in two different Hardware Description Language (HDL)-based codes, i.e. VerilogA [1, 2] and SpectreHDL [3], within the Cadence Integrated Circuits (ICs) development environment (www.cadence.com), for the Spectre Circuit Simulator [4, 5]. As mentioned before, the tool can be ported in other simulation environments, i.e. alternative to Cadence, as long as HDL codes are supported.

All the most important issues, including the proper configuration of the library itself within the Cadence environment, the properties settings of each model together with the practical use of the tool, e.g. simple examples of MEMS structures and clues about how to face convergence difficulties, will be covered through the following pages.

Moreover, the library being available in two different HDL based codes, different details depending on the particular implementation will be kept and explained separately, both for the VerilogA and the SpectreHDL version.

B.2 How to configure the software library within the Cadence environment

The MEMS compact model library is treated by Cadence as a standard design kit. This means that it has to be copied in a proper location of the file system, which we define here to be `/users/OPUS`. If we now name the two libraries as `MEMS_MODELER_CONTAINER_VerilogA` and `MEMS_MODELER_CONTAINER_SpectreHDL`, the components within each of them will be seen as subdirectories

addressed by the following paths: `/users/OPUS/MEMS_MODELER_CONTAINER_VerilogA` and `/users/OPUS/MEMS_MODELER_CONTAINER_SpectreHDL`.

The previous absolute paths must then be added to the **Library Path Editor** [5] within Cadence, in order to make the two libraries visible and usable within the software, together with the other pre-existing libraries and design kits, as reported in figure B.1.

The MEMS compact models deal with mixed-domain magnitudes, i.e. electrical and mechanical. Proper definitions for the electrical and mechanical magnitudes are declared within the libraries. For each of the two parameters, i.e. **abstol** and **blowup**

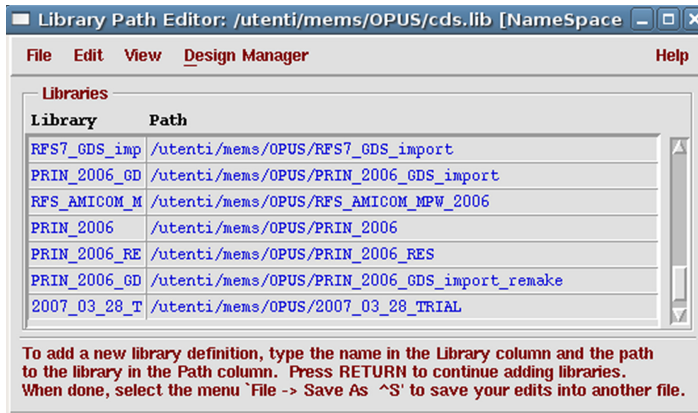


Figure B.1. Library Path Editor window in Cadence. Once the library definitions are added, the new configuration must be saved in the `cds.lib` file.

Table B.1. Summary of all the electrical and mechanical magnitudes' definitions within the VerilogA and SpectreHDL library versions.

Name within Cadence	Physical meaning	Unit	abstol	blowup
disp	Mechanical linear displacement	Meter (m)	1.0e-9	
frc	Mechanical linear force	Newton (N)	1.0e-9	
vel	Mechanical linear velocity	Meter/Second (m s ⁻¹)	1.0e-3	1.0e+12
acc	Mechanical linear acceleration	Meter/Second ² (m s ⁻²)	1.0e-3	1.0e+12
ang	Mechanical rotation	Radian (rad)	1.0e-3	
trq	Mechanical torque	Newton*Meter (N*m)	1.0e-3	
avel	Mechanical angular velocity	Radian/Second (rad s ⁻¹)	1.0e-3	1.0e+12
aacc	Mechanical angular acceleration	Radian/Second ² (rad s ⁻²)	1.0e-3	1.0e+12
V	Voltage	Volts (V)	1.0e-6	1.0e+12
I	Current	Ampere (I)	1.0e-6	1.0e+12

[2, 3], threshold values are defined for all the magnitudes that are necessary to the Spectre simulator to discriminate convergence and non-convergence conditions. All the magnitudes with their physical meaning, name within Cadence, unit and parameter(s) value(s) are listed in table B.1.

In the VerilogA library the implementation definitions listed in table B.1 are included in the file `/users/OPUS/MEMS_MODELER_CONTAINER_VerilogA/discipline/discipline.h` and no special settings are required to properly link such a file.

In the SpectreHDL the implementation information listed in table B.1 are defined within the file `/users/OPUS/MEMS_MODELER_CONTAINER_SpectreHDL/quantity.spectre`.

This file must be linked to make it visible during simulations. To do so, a line containing the information on where the file is located must be added to the `cds.lib` file (absolute path: `/users/OPUS/cds.lib`) before the lines referring to the actual libraries and loaded design kits. In this case, the line has to be as follows: `DEFINE MEMS_MODELER_CONTAINER_SpectreHDL /users/OPUS/MEMS_MODELER_CONTAINER_SpectreHDL`.

B.3 How to instance the available components

Each component within the library is identified by a schematic symbol. This allows one to compose the object to be simulated by adding instances within a Cadence Composer Schematic window, as is usually done with standard libraries of semiconductor devices, and as is shown in figures B.2 and B.3.

Then, the components instanced within the schematic are connected together by means of wires, as reported in figure B.4.

B.4 The flexible straight deformable beam

This section describes how to set all the parameters of the flexible straight beam model, previously discussed in section 5.2.2. Custom configurations of the components are possible, depending on the type of simulation that must be performed. The selection of features is going to be shown below. Any time a change is performed, the component code must be recompiled, in order to allow Spectre to generate the

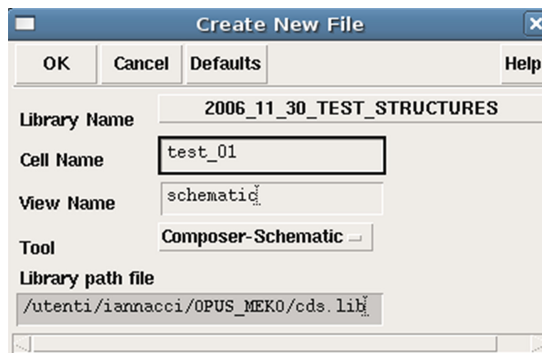


Figure B.2. Definition of a new Composer Schematic file within an existing library.

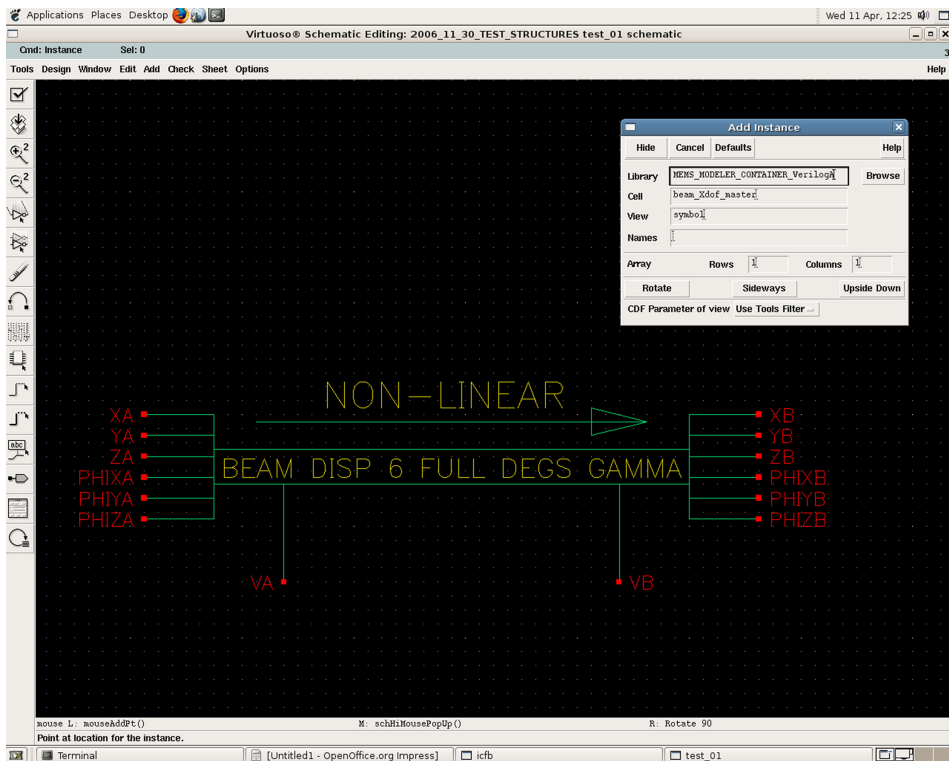


Figure B.3. Instantiation of MEMS elementary components within the schematic window.

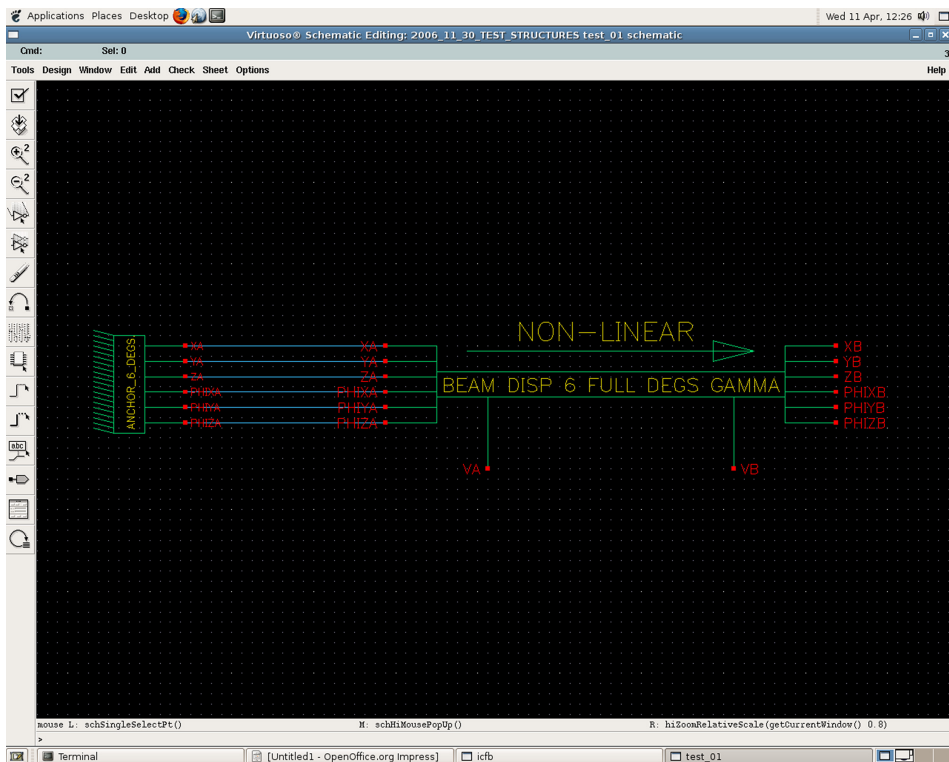


Figure B.4. Connection of single components through wires.

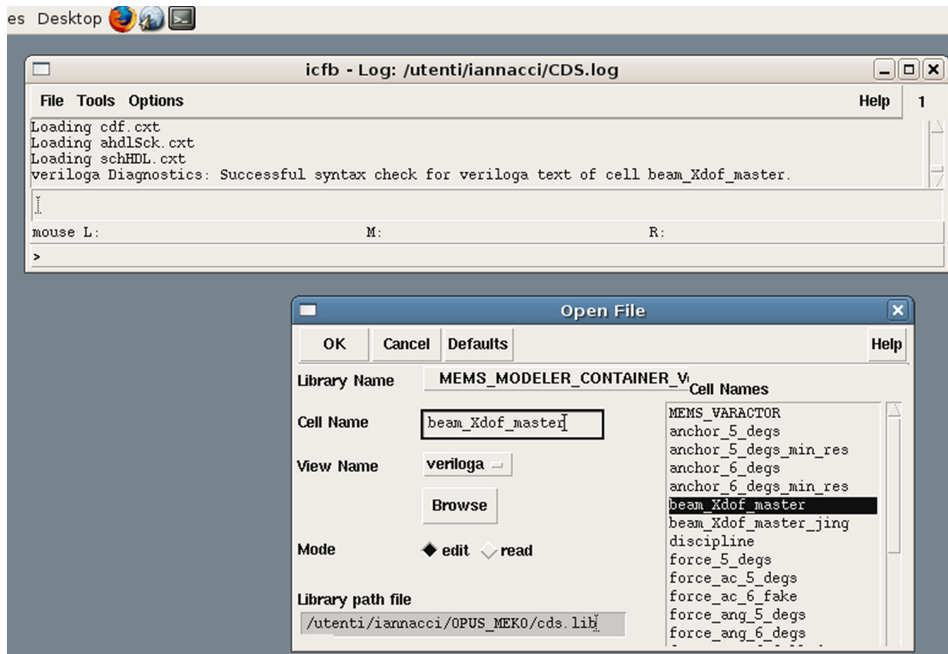


Figure B.5. Opening of the main code file for the 12 DoF flexible beam. In the case of the SpectreHDL implementation the **View Name ahdl** has to be selected.

proper netlist, necessary for the simulation. This means that the main code file must be opened and saved within Cadence. Each component is defined in a subdirectory within the library. The 12 Degrees of Freedom (DoF) straight beam subfolder is named **beam_Xdof_master** for both the library implementations. The main code file for the VerilogA and SpectreHDL is respectively located in the subsequent absolute paths: **/users/OPUS/MEMS_MODELER_CONTAINER_VerilogA/beam_Xdof_master/veriloga/veriloga.va** and **/users/OPUS/MEMS_MODELER_CONTAINER_SpectreHDL/beam_Xdof_master/ahdl/ahdl.def**.

Such files can be opened from the main Cadence window (**File** → **Open**) selecting the proper **View Name** (**veriloga** or **ahdl**) depending on the implementation. The case of the VerilogA implementation is shown in figure B.5.

In response, a text editor window will open (usually the **vi** Unix Editor). By saving and closing such a file, the compilation will be automatically launched. In the case of **vi** the command to be typed is **:wq + Enter**, i.e. write and quit, as shown in figure B.6.

B.4.1 Features definitions

The list of all the possible features is contained in the file with absolute path: **/users/OPUS/MEMS_MODELER_CONTAINER_VerilogA/beam_Xdof_master/main/main_beam.rgd**, and its content is reported below:

```

/utenti/iannacci/MEMS_MODELER_CONTAINER_VerilogA, - □ ×
// VerilogA for modelli, beam_Xdof_master_nuova_veriloga, veriloga
// *****
// Jacopo Iannacci 08/09/2004
// Last Extention 21/10/2004
// Version 3,2,0
// *****
// Implementation of a Simple flexible beam (small deflexions)
// with respect to the x, y, z axis and rotation phi around the x, y and z axis
// 6 degrees of freedom
// It is not possible give an initial value for rotation's angle around the x-axis
// because it's impossible in the layout.
// In this version the rotation angles around the x, y and z-axis are
// also transformed
// into the local reference's system

`include "../discipline/discipline.h"

`define MIN_ANG_X +1.0e-1

`define MIN_ANG_Y +1.0e-6
:wq

```

Figure B.6. The command `:wq + Enter`, i.e. write and quit, launches the compilation of the file with the new features selection.

```

/// ***** ///
/// MODULES INCLUSION. DEFINITION OF A CUSTOM BEAM MODEL FOR
SIMULATIONS. ///
/// ***** ///
// If parameters values are set to 1, the corresponding
module is included
// in the beam model, otherwise, if the value is equal to 0,
it is not included
//`define Rotation_Matrix_Modified
//`define Non_Linear_Deformations
//`define DC_Simulation_Model_Reduction
`define Shear_Effects
`define Contact_Effects
`define Electrostatic_Force
`define Capacitance
`define Apart_Electrodes
//`define No_Torsion_Around_X
`define Viscous_Damping
/// ***** ///
///————— END OF THE MODULES INCLUSION ————— ///
/// ***** ///

```

The file contains a series of **macro** variables definition. When a variable is defined, it assumes a **TRUE** value (which means that the corresponding line is not commented,

i.e. it does not begin with the comment operator `//`), and the corresponding feature is included in the code compilation. Whereas when a variable is commented it is not defined, and consequently the compiler query returns a **FALSE** value. In this case, the feature defined by that variable will not be included in the model.

For the SpectreHDL implementation, the file is located at the following absolute path: `/users/OPUS/MEMS_MODELER_CONTAINER_SpectreHDL/beam_Xdof_master/main/main_beam.rgd` and its content is reported below:

```

/// ***** //
/// MODULES INCLUSION. DEFINITION OF A CUSTOM BEAM MODEL FOR
SIMULATIONS. ///
/// ***** //
// If parameters values are set to 1, the corresponding
module is included
// in the beam model, otherwise, if the value is equal to 0,
it is not included
#define Rotation_Matrix_Modified 0
#define Non_Linear_Deformations 0
#define DC_Simulation_Model_Reduction 0
#define Shear_Effects 1
#define Contact_Effects 1
#define Electrostatic_Force 1
#define Capacitance 1
#define Apart_Electrodes 1
#define No_Torsion_Around_X 0
#define Viscous_Damping 1
/// ***** //
/// ----- END OF THE MODULES INCLUSION ----- //
/// ***** //

```

In this case, a numeric value is associated to each **macro** variable definition, i.e. **0 = FALSE** and **1 = TRUE**. It has to be stressed that, in order to simplify the explanation, the configuration of the main inclusion file is the same for the two VerilogA and SpectreHDL implementations of the 12 DoF beam. The variables are now discussed and explained in detail, one by one, as listed in table [B.2](#).

When the features selection corresponds to the one shown above in the `main_beam.rgd` file (for both the VerilogA and SpectreHDL implementations), the parameters accessible through the **Edit Object Properties** windows (reachable by selecting the beam schematic and typing **Q**), are reported in figure [B.7](#).

A detailed explanation of each parameter reported in figure [B.7](#) is provided in the table [B.3](#).

NOTE: Misunderstandings can rise among orientation angles values within the mask in figure [B.7](#) and the position of the beam schematic in the Composer windows of Cadence (previously reported in figure [B.3](#)). To this end, it has to be stressed that whatever rotation of the schematic does not imply a corresponding rotation of the beam

Table B.2. Summary of all the features that can be modified in the 12 DoF beam model.

Variable name	Corresponding feature
Rotation_Matrix_Modified	Defines a different analytical implementation for the rotation matrix compatible with large deformations [6]. NOTE: This feature is not tested and the variable should be left to the FALSE value.
Non_Linear_Deformations	Defines an analytical implementation accounting for the material non-linearities when large deformations occur [6]. NOTE: This feature is not tested and the variable should be left to the FALSE value. In most cases, the beam deformations are small enough to make the linear mechanical model still suitable to reach a good predictive accuracy.
DC_Simulation_Model_Reduction	When set to TRUE , it cuts out the compilation of all the dynamic nodes' definitions (i.e. time derivatives). NOTE: This feature makes the model more robust against convergence problems. However, it can be used only for static DC simulations, as all the dynamics due to inertia and viscous damping are ignored.
Shear_Effects	When set to TRUE , it includes the shear effects in the linear mechanical model [7]. NOTE: It should be always set TRUE .
Contact_Effects	When set to TRUE , it includes the presence of the substrate underneath the beam, i.e. includes the collapse (pull-in) of the beam onto the substrate. NOTE: If set to FALSE , none of the features that are following can be included.
Electrostatic_Force	When set to TRUE , it includes the electrostatic attractive force between the beam and the substrate, when a bias voltage is applied between them.
Capacitance	When set to TRUE , it enables the calculation of the capacitance between the suspended beam and the underlying substrate.
Apart_Electrodes	When set to TRUE , enables the definition of separated electrodes along the beam length (refer to [8], their appendix B, for more details).
No_Torsion_Around_X	When set to TRUE , it ignores the torsion around the X axis along the beam length, both in the electrostatic magnitudes calculations and in the viscous damping effect model. NOTE: It can be reasonably left FALSE as torsions around the X axis are usually small, reducing the computational complexity of the model.
Viscous_Damping	When set to TRUE , it includes the dynamic effect of the squeeze film damping, which counteracts the beam movements [9].

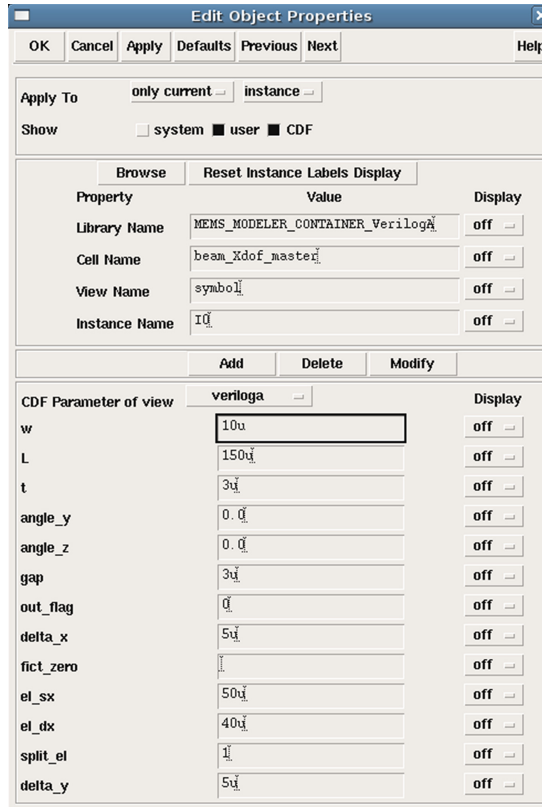


Figure B.7. Object Properties mask of the 12 DoF flexible beam with the features described above in the `main_beam.rgd` file. In the case of SpectreHDL, the CDF Parameter of view `ahdl` must be chosen.

Table B.3. Summary of all the parameters in the 12 DoF beam properties mask.

Parameter	Meaning
w	Beam width along the <i>Y</i> axis (see section 5.2.2). In the case, as reported in figure B.7, it is 10 μm .
L	Beam length along the <i>X</i> axis.
t	Beam thickness along the <i>Z</i> axis.
angle_y	Initial beam orientation angle (in degrees) around the <i>Y</i> axis.
angle_z	Initial beam orientation angle (in degrees) around the <i>Z</i> axis.
gap	Vertical distance between the suspended beam and the underlying substrate (i.e. air gap).
out_flag	Boolean flag. If set to 1 (TRUE) , real-time information about the electrostatic force and capacitance values are displayed during the simulation.
delta_x	In the electrostatic magnitudes calculation the beam length is discretised into an integer number of rigid non-parallel plates (see section 5.2.2). The parameter delta_x defines the length of each of these elements.

(Continued)

Table B.3. (Continued)

Parameter	Meaning
fict_zero	Value considered as fictitious zero in order to avoid division by zero. NOTE: When nothing is specified in the mask, it is set to 1e-6 by default. This value usually does not need to be modified.
el_sx	Defines the length of the left-hand portion of the electrode (refer to [8], their appendix B, for more details).
el_dx	Defines the length of the right-hand portion of the electrode (refer to [8], their appendix B, for more details).
split_el	Defines the splitting scheme of the electrodes determined by the previous two parameters (refer to [8], their appendix B, for more details). When split_el = 1 , the electrode is placed in the area not covered both from el_sx and el_dx . Alternatively, when split_el = 0 , the electrode is placed on the area covered by el_sx and el_dx .
delta_y	This parameter is similar to delta_x , but it defines the sub-elements length along the Y axis.

within the structure to be simulated. In fact, such rotations are defined by means of the **angle_y** and **angle_z** parameters defined above in table B.3. In light of this, maintaining a logic link between the orientation of the symbol instanced within the schematic and the values of the latter parameters can help. For instance, if **angle_z = 90°**, the beam schematic should be rotated 90° counter clockwise. Differently, if **angle_z = -90° = 270°**, the beam schematic should be rotated 90° clockwise.

B.4.2 Materials' characteristics

Materials' properties, likewise several other constants, can be modified to adapt the beam model to the technology specifications. In both the VerilogA and SpectreHDL implementations, a header file exists defining which other files containing the technology and constants definitions must be included. The absolute paths of such header files are: **/users/OPUS/MEMS_MODELER_CONTAINER_VerilogA/qunatities/quantities.tf** and **/users/OPUS/MEMS_MODELER_CONTAINER_SpectreHDL/qunatities/quantities.tf**.

In the following, only the case of the VerilogA implementation is going to be shown, as the approach is the same for the SpectreHDL version. The content of the file **quantities.tf** follows:

```
// ***** //
// —CONSTANTS— //
// ***** //
`include "constants.tf"
// ***** //
// ————END——— //
// ***** //
// ***** //
```

```

// —PHYSICAL QUANTITIES— //
// ***** //
`include "air.tf"
// ***** //
// —————END————— //
// ***** //
// ***** //
// —TECHNOLOGY FILE— //
// ***** //
//`include "./tech/irst.tf"
//`include "./tech/poly.tf"
`include "./tech/irst_new.tf"
//`include "./tech/philips_04_06_2004.tf"
// ***** //
// —————END————— //
// ***** //

```

The first two inclusions are for the **constants.tf** and **air.tf** files, which are located in the same subfolder of **quantities.tf**. They define some constants and the air's characteristic values (e.g. viscosity and permittivity), respectively. For instance, if one is interested in simulating MEMS structures within a nitrogen atmosphere instead of air, the values within **air.tf** are to be modified, or a new file (e.g. **nitrogen.tf**) containing the proper values has to be created within the current subfolder and then included in **quantities.tf** (with the line `'include 'nitrogen.tf'`).

Concerning the technology file with materials information, four of them are declared within **quantities.tf**, despite just one of them being chosen (in this case **irst_new.tf**). The technology files are located in the following path: **/users/OPUS/MEMS_MODELER_CONTAINER_VerilogA/quantities/tech/**. The content of **'irst_new.tf'** is the following:

```

//////////////////////////////////// GOLD VALUES //////////////////////////////////////
rho= 0.005;// Structural layer sheet resistance ohm/square.
E=98.5e9;// Young's modulus (Pascal).
dens=19300.0;// Density (kg/m^3).
Poi_nu=0.42;// Poisson's ratio.
thox=100.0e-9;// Oxide thickness above the bottom plate.
erox=5.7;// Oxide dielectric constant.
rough_air_spacer=0;// Extra air gap due to the oxide
roughness.
K_touch=10.0G;// Fictitious elastic parameter when collision
occurs.
min_dist = 10.0e-6;// Minimum distance of two hole on the
plate surface.
Stat_damp = 9.0e-2;// Static damping coefficient.
Dyna_damp = 2.0e-2;// Dynamic damping coefficient.
////////////////////////////////////

```

Table B.4. Summary of all the technology parameters within the `irst_new.tf` file.

Parameter name	Definition and physical magnitude
rho	Sheet resistance of the gold structural layer (Ω/sq).
E	Young's modulus of gold (Pa).
dens	Density of gold (Kg/m^3).
Poi_nu	Poisson's ratio of gold.
thox	Thickness of the insulating silicon oxide layer deposited above the bottom electrode (m).
erox	Relative dielectric constant of the silicon oxide (F/m).
rough_air_spacer	Effective value of the silicon oxide surface roughness (m). NOTE: This parameter defines the residual air gap due to the surface roughness when the pull-in condition is reached.
K_touch	Fictitious elastic constant defining the lower contact plane when pull-in occurs (N/m).
min_dist	Minimum distance between two adjacent holes placed on the beam surface (m). NOTE: This feature is not used in the beam model, as it mainly refers to the rigid plate (see next pages).
Stat_damp	Static friction coefficient when collision occurs. NOTE: It is not used in the beam model, as it mainly refers to the rigid plate (see next pages).
Dyna_damp	Dynamic friction coefficient when collision occurs ($\text{N}^*\text{s m}^{-1}$). NOTE: It is not used in the beam model, as it mainly refers to the rigid plate (see next pages).

The meaning and explanation of each parameter listed above is summarised in table B.4.

When a new technology has to be defined, it is possible either to modify the values of an existing file (like `irst_new.tf`), or to create a new file within the folder `/users/OPUS/MEMS_MODELER_CONTAINER_VerilogA/quantities/tech/`, and then by including it in the `quantities.tf` header file (the latter solution being more straightforward).

NOTE: Every time a value is modified (in the constants or in the technology part), the model must be recompiled (as reported in figures B.5 and B.6) in order to make the change(s) effective.

B.5 The rigid plate suspended electromechanical transducer

Following the same approach of the previous section, the current section focuses on the rigid plate electromechanical transducer model. All the details concerning the mathematical formulation, the physical features and the working principles of the MEMS transducer were previously reported and discussed in section 5.2.1.

Whatever is concerned with the materials' and general properties' definitions was already covered in the previous section on the flexible straight beam. Therefore, such information will not be duplicated in this section, as they still hold validity for the rigid plate model.

B.5.1 Features definition

The name of the subfolder containing the plate model is **plate_Xdof_master** in both the VerilogA and SpectreHDL implementations. The list of all the possible features is contained in the files with the absolute paths: **/users/OPUS/MEMS_MODELER_CONTAINER_VerilogA/plate_Xdof_master/main/main_plate.rgd** and **/users/OPUS/MEMS_MODELER_CONTAINER_SpectreHDL/plate_Xdof_master/main/main_plate.rgd**.

The content of the file with all the selectable features, for only the case of VerilogA implementation, is reported in the following:

```
// _____ //
//`define Model_Reduction_To_4_Degrees_Of_Freedom
// _____ //
//`define Rotation_Matrix_Modified
`define Offset_Connectivity_Point
`define Contact_Effects
//`define In_Plane_Contact_Effects_Static
//`define In_Plane_Contact_Effects_Dynamic
// _____ //
`define Straight_Lines
`define Oxide_Electrical_Effects
`define Electrical_Effects_Capacitance
`define Electrical_Effects_Force
`define Boundary_Fringing_Capacitance
`define Boundary_Fringing_Electrostatic
`define Lateral_Fringing_Capacitance_Integral
`define Lateral_Fringing_Electrostatic_Integral
`define Manual_Holes_Placement
`define Holes_Capacitance
`define Holes_Electrostatic
`define Holes_Boundary_Fringing_Capacitance
`define Holes_Boundary_Fringing_Electrostatic
`define Holes_Lateral_Fringing_Capacitance_Integral
`define Holes_Lateral_Fringing_Electrostatic_Integral
//`define Electrostatic_Torques
// _____ //
`define Viscous_Damping_Effects
//`define Simplified_Viscous_Damping_Model
//`define Viscous_Damping_Torques_Model
//`define Simplified_Viscous_Damping_Torques_Model
//`define Discrete_Damping_Model
`define Mean_Free_Path_Model
// _____ //
//`define DC_Simulation_Model_Reduction
```

```

`define Torque_Nodes_Static_Damping_Inclusion
`define Torque_Nodes_Dynamic_Damping_Inclusion
`define Center_Of_Mass_Dynamic_Nodes_For_X
`define Center_Of_Mass_Dynamic_Nodes_For_Y
`define Center_Of_Mass_Dynamic_Nodes_For_Z
`define Center_Of_Mass_Dynamic_Nodes_For_Phi_X
`define Center_Of_Mass_Dynamic_Nodes_For_Phi_Y
`define Center_Of_Mass_Dynamic_Nodes_For_Phi_Z
// _____ //

```

The meaning and description of all the rigid plate features reported above is listed in table B.5.

The properties mask associated with the rigid plate Cadence symbol is shown in figure B.8. The meaning and description of all the parameters is listed in table B.6 and they correspond to the configuration of the **main_plate.rgd** file shown in the previous pages.

B.6 Complementary components

In this section, all the complementary components included in the library, and necessary to impose mechanical boundary conditions and provide stimuli, are briefly described. Such components, along with the symbols in Cadence, were already introduced and shown in section 5.2.3, to which the reader can refer for more details. The mentioned elements are going to be reviewed here from a more practical and operational point of view. The complementary components can be grouped in two categories, i.e. boundary conditions and stimulus sources, as reported in the following.

B.6.1 Anchoring point—boundary condition component

This device imposes a mechanical constraint to all the linear and angular DoFs, realising an anchoring point. Each of its nodes does not allow any displacement or rotation to the device connected to it. The 6 DoF anchoring element subfolder name within both libraries is **anchor_6_degs**, and the Cadence schematic symbol is shown in figure 5.22 in the previous chapter 5.

B.6.2 Anchoring point with minimum resistance—boundary condition component

When the anchoring point has to be connected to a rigid body (i.e. suspended rigid plate), it is similar to shorting together two voltage generators in the electrical domain. This case cannot be managed by the Spectre simulator and an error occurs. To avoid this condition, an on-purpose anchoring element is available within both libraries. It is called **anchor_6_degs_min_res** and the Cadence schematic symbol is shown in figure 5.23, in the previous chapter 5. The element at stake features a minimum resistance value defined within the model, preventing from the error condition mentioned above. The parameter **r_min** is accessible through the

Table B.5. Description of all the possible features related to the rigid plate suspended electromechanical transducer model.

Parameter name	Meaning
<hr/> Mechanical model <hr/>	
Model_Reduction_To_4_Degrees_Of_Freedom	##### When set to TRUE , it reduces the plate mechanical model to 4 Degrees of Freedom (DoFs) (three linear displacements and a rotation allowed only around the vertical <i>Z</i> axis). This means that the plate is always parallel to the substrate. When set to FALSE , the plate admits any position in space (6 DoFs, i.e. three linear displacements and rotations around the three axes <i>X</i> , <i>Y</i> , <i>Z</i>).
<hr/> Plate features <hr/>	
Rotation_Matrix_Modified	##### It defines a different analytical implementation for the rotation matrix compatible with large deformations [6]. NOTE: This feature is not tested and the variable should be always set to FALSE .
Offset_Connectivity_Point	When set to TRUE , it allows displacing the four interconnection points between the plate and the external world with respect to the four plate corners North-East (NE), South-East (SE), South-West (SW) and North-West (NW) (refer to [8], their appendix A, for more details).
Contact_Effects	When set to TRUE , it accounts for the presence of the substrate underneath the plate, i.e. it makes possible the collapse of the plate on the substrate (pull-in). NOTE: When set to FALSE , none of the following features can be included.
In_Plane_Contact_Effects_Static	When set to TRUE , it includes the <i>XY</i> in-plane static friction between the plate and the substrate when physical collision occurs. NOTE: The accuracy of this feature is not verified and it might lead to convergence issues. Moreover, such an effect is usually not dominant in standard RF-MEMS switch topologies. Therefore, this feature can be kept FALSE .
In_Plane_Contact_Effects_Dynamic	When set to TRUE , it includes the <i>XY</i> in-plane dynamic (sliding) friction between the plate

(Continued)

Table B.5. (Continued)

Parameter name	Meaning
	and the substrate when physical collision occurs. NOTE: The accuracy of this feature is not verified and it might lead to convergence issues. Moreover, such an effect is usually not dominant in standard RF-MEMS switch topologies. Therefore, this feature can be kept FALSE .
Electrostatic effects	#####
Straight_Lines	When set to TRUE , the electric field lines between the plate and the substrate are approximated to straight instead of curved lines. NOTE: When the plate mechanical model is reduced to 4 DoFs, the field lines are always straight. Instead, when dealing with the 6 DoF model, it might happen very rarely that the curved lines model causes convergence issues. In this case, it can be set to TRUE . The error increase in electrostatic force and capacitance calculations due to straight line approximation is generally rather small.
Oxide_Electrical_Effects	When set to TRUE , the electrical effects due to the oxide layer laying on the lower substrate are accounted. The air gap and the oxide layer are treated as two series capacitances (refer to [8], their appendix A, for more details).
Electrical_Effects_Capacitance	When set to TRUE , it includes the calculation of the capacitance between the suspended plate and the substrate.
Electrical_Effects_Force	When set to TRUE , it includes the calculation of the attractive electrostatic force between the suspended plate and the substrate.
Boundary_Fringing_Capacitance	When set to TRUE , the fringing capacitance due to the distortion of the field lines nearby the plate's four edges is included in the capacitance calculation (refer to [8], their appendix A, for more details).
Boundary_Fringing_Electrostatic	When set to TRUE , the fringing electrostatic force due to the distortion of the field lines nearby the plate's four edges is included in the attractive force calculation (refer to [8], their appendix A, for more details).

Lateral_Fringing_Capacitance_Integral	When set to TRUE , the fringing capacitance due to the field lines starting from the four plate boundary vertical sidewalls is included in the capacitance calculation (refer to [8], their appendix A, for more details). NOTE: When the plate is parallel to the substrate, this contribution is null.
Lateral_Fringing_Electrostatic_Integral	When set to TRUE , the fringing electrostatic force due to the field lines starting from the four plate boundary vertical sidewalls is included in the attractive force calculation (refer to [8], their appendix A, for more details). NOTE: When the plate is parallel to the substrate, this contribution is null.
Manual_Holes_Placement	When set to TRUE , the distance between the most peripheral holes' edges and the plate boundaries can be defined by the user (refer to figure 13 in chapter 5). Otherwise, the hole-to-edges clearance is automatically defined.
Holes_Capacitance	When set to TRUE , it includes the presence of holes on the plate surface and calculates the actual capacitance value affected by the holes. NOTE: When set to TRUE , the presence of holes is automatically accounted for in the mechanical plate model (inertia) and in the viscous damping model, as well.
Holes_Electrostatic	When set to TRUE , it includes the presence of holes on the plate surface and calculates the actual electrostatic force value affected by the holes. NOTE: When set to TRUE , the presence of holes is automatically accounted in the mechanical plate model (inertia) and in the viscous damping model as well.
Holes_Boundary_Fringing_Capacitance	When set to TRUE , the fringing capacitance due to the distortion of the field lines nearby the holes' edges is included in the capacitance calculation (refer to [8], their appendix A, for more details).
Holes_Boundary_Fringing_Electrostatic	When set to TRUE , the fringing electrostatic force due to the distortion of the field lines nearby the holes' edges is included in the attractive force calculation (refer to [8], their appendix A, for more details).

(Continued)

Table B.5. (Continued)

Parameter name	Meaning
Holes_Lateral_Fringing_Capacitance_Integral	When set to TRUE , the fringing capacitance due to the field lines starting from the holes' vertical sidewalls is included in the capacitance calculation (refer to [8], their appendix A, for more details). NOTE: When the plate is parallel to the substrate, this contribution is null.
Holes_Lateral_Fringing_Electrostatic_Integral	When set to TRUE , the fringing electrostatic force due to the field lines starting from the holes' vertical sidewalls is included in the attractive force calculation (refer to [8], their appendix A, for more details). NOTE: When the plate is parallel to the substrate, this contribution is null.
Electrostatic_Torques	When set to TRUE , the torque due to the attractive electrostatic force (occurring when the plate is not parallel to the substrate) is calculated (refer to [8], their appendix A, for more details). NOTE: The electrostatic torque contribution is usually very small and can be excluded from the model without significant loss in predictive accuracy.
—————Viscous damping effect—————	#####
Viscous_Damping_Effects	When set to TRUE , it includes the viscous damping effect in the rigid plate model. NOTE: When Holes_Capacitance or Holes_Electrostatic are set to TRUE , the viscous damping model accounts for the holes. Otherwise, the plate is considered without openings on its surface.
Simplified_Viscous_Damping_Model	This parameter addresses a simplified mathematical implementation of the viscous damping model, in case holes are not present on the plate surface. NOTE: When the plate is set without holes, it is better to select the simplified model as it allows considerable simulation time saving, without introducing significant loss in predictive accuracy.
Viscous_Damping_Torques_Model	When set to TRUE , it includes the calculation of the torque due to the viscous damping effect. NOTE: This contribution is not dominant, therefore it can be reasonably neglected in the model definition.

Simplified_Viscous_Damping_Torques_Model	This parameter considers a simplified mathematical implementation of the viscous damping torque calculation. NOTE: This contribution is not dominant, therefore it can be reasonably neglected in the model definition.
Discrete_Damping_Model	This parameter considers a discrete implementation of the viscous damping effect, when there are no holes on the plate surface. NOTE: Since Simplified_Viscous_Damping_Model is a better choice when there are no holes, this feature can be always kept FALSE .
Mean_Free_Path_Model	When set to TRUE , it includes the calculation of an effective fluid viscosity (according to the model proposed by Veijola in [10]). NOTE: Since the so-called slip-flow becomes dominant when the air gap is very small (i.e. same order of magnitude of the gas molecules' mean free path), this feature must be included every time the pull-in is expected to be reached.
<hr style="width: 30%; margin-left: 0;"/> DC_Simulation_Model_Reduction	<p>#####</p> <p>When set to TRUE, it cuts out of the compilation all the dynamic nodes' definitions (i.e. time derivatives). NOTE: It makes the model more robust against convergence issues, even though it can be used only for static DC simulations, as all the dynamics due to inertia and viscous damping are ignored.</p>
Torque_Nodes_Static_Damping_Inclusion	This parameter includes internal nodes for the static <i>XY</i> in-plane friction. It must be set to TRUE when In_Plane_Contact_Effects_Static is TRUE .
Torque_Nodes_Dynamic_Damping_Inclusion	This parameter includes internal nodes for the dynamic <i>XY</i> in-plane friction. It must be set to TRUE when In_Plane_Contact_Effects_Dynamic is TRUE .
Center_Of_Mass_Dynamic_Nodes_For_X	When set to FALSE , it does not include all the dynamic nodes (velocity and acceleration) for the <i>X</i> axis linear displacement DoF. NOTE: This parameter may be used to increase the convergence robustness, despite

(Continued)

Table B.5. (Continued)

Parameter name	Meaning
Center_Of_Mass_Dynamic_Nodes_For_Y	<p>it cutting off all the dynamic effects (inertia and viscous damping) related to the X axis linear displacement DoF.</p> <p>When set to FALSE, it does not include all the dynamic nodes (velocity and acceleration) for the Y axis linear displacement DoF.</p> <p>NOTE: This parameter may be used to increase the convergence robustness, despite it cutting off all the dynamic effects (inertia and viscous damping) related to the Y axis linear displacement DoF.</p>
Center_Of_Mass_Dynamic_Nodes_For_Z	<p>When set to FALSE, it does not include all the dynamic nodes (velocity and acceleration) for the Z axis linear displacement DoF.</p> <p>NOTE: This parameter may be used to increase the convergence robustness, despite it cutting off all the dynamic effects (inertia and viscous damping) related to the Z axis linear displacement DoF.</p>
Center_Of_Mass_Dynamic_Nodes_For_Phi_X	<p>When set to FALSE, it does not include all the dynamic nodes (velocity and acceleration) for the rotation around the X axis DoF.</p> <p>NOTE: This parameter may be used to increase the convergence robustness, despite it cutting off all the dynamic effects (inertia and viscous damping) related to the rotation around the X axis DoF.</p>
Center_Of_Mass_Dynamic_Nodes_For_Phi_Y	<p>When set to FALSE, it does not include all the dynamic nodes (velocity and acceleration) for the rotation around the Y axis DoF.</p> <p>NOTE: This parameter may be used to increase the convergence robustness, despite it cutting off all the dynamic effects (inertia and viscous damping) related to the rotation around the Y axis DoF.</p>
Center_Of_Mass_Dynamic_Nodes_For_Phi_Z	<p>When set to FALSE, it does not include all the dynamic nodes (velocity and acceleration) for the rotation around the Z axis DoF.</p> <p>NOTE: This parameter may be used to increase the convergence robustness, despite it cutting off all the dynamic effects (inertia and viscous damping) related to the rotation around the Z axis DoF.</p>



Figure B.8. Cadence window highlighting all the rigid plate properties that can be set by the user.

Table B.6. Description of all the parameters available in the plate schematic properties mask within Cadence.

Parameter	Meaning
w	Width of the rigid plate along the X axis (refer to section 5.2.1 for more details). In this case, $w = 220 \mu\text{m}$ (see figure B.8).
L	Length of the rigid plate along the Y axis (see figure B.8).
t	Thickness of the rigid plate along the Z axis (see figure B.8).
angle_z	Plate initial rotation angle around the Z axis (expressed in degrees) (see figure B.8).
gap	Vertical distance between the suspended plate and the underlying substrate. NOTE: The gap includes also the thickness of the insulating layer laying above the substrate.
fa	The parameter fringing arc (fa) defines the curvature of the fringing field lines nearby the plate edges (refer to [8], their appendix A, for more details). It varies within the interval [0,1]. The larger it is, the more the field lines are curved. NOTE: The fa parameter was tuned by means of Finite Element Method (FEM) simulations and it can be set to 0.25 [8, 11].
fw	The parameter fringing width (fw) defines the area nearby the plate edges within which the fringing effect is supposed to be confined (refer to [8], their appendix A, for more details). NOTE: The fw parameter was tuned with FEM simulations and it can be set to 100 nm [8, 11].
sp_x_lft	Clearance (along the X axis) between the left plate edge and the left edge of the first holes column (refer to figure 13 in chapter 5).
sp_x_rgt	Clearance (along the X axis) between the right plate edge and the right edge of the last holes column (refer to figure 13 in chapter 5).
sp_y_bot	Clearance (along the Y axis) between the bottom plate edge and the bottom edge of the lowest holes row (refer to figure 13 in chapter 5).
sp_y_top	Clearance (along the Y axis) between the top plate edge and the top edge of the highest holes row (refer to figure 13 in chapter 5).
nhl_x	Number of holes (integer) along the X axis.
nhl_y	Number of holes (integer) along the Y axis.
hl_x	Holes width along the X axis (refer to figure 13 in chapter 5).
hl_y	Holes length along the Y axis (refer to figure 13 in chapter 5).
fah	The parameter fringing arc holes (fah) defines the curvature of the fringing field lines nearby the holes' edges. It varies within the interval]0,1]. The larger it is, the more curved the field lines are (refer to fa). NOTE: The fah parameter was tuned with FEM simulations and in can be kept to 0.25 [8, 11].
fwh	The parameter fringing width holes (fwh) defines the area nearby the holes' edges, within which the fringing effect is supposed to be confined (refer to fw). NOTE: The fwh parameter was tuned with FEM simulations and it can be kept to 100 nm [8, 11].
fal	The parameter fringing arc lateral (fal) defines the curvature of the fringing field lines nearby the plate vertical sidewalls (refer to [8], their appendix A, for more details). It swings within the interval]0,1]. The larger it is, the more curved the field lines are. NOTE: The fal parameter was tuned with FEM simulations and it can be kept to 0.25 [8, 11].

falh	The parameter fringing arc lateral holes (falh) defines the curvature of the fringing field lines nearby the vertical sidewalls of holes. It varies within the interval]0,1]. The larger it is, the more curved the field lines are (refer to fal). NOTE: The falh parameter was tuned with FEM simulations and it can be kept to 0.25 [8, 11].
out_flag	Boolean flag. If set to 1 , real-time information about the electrostatic force and capacitance values are displayed during simulations.
angle_x	Plate initial rotation angle around the <i>X</i> axis (expressed in degrees) (refer to the images in section 5.2.1 for more details).
angle_y	Plate initial rotation angle around the <i>Y</i> axis (expressed in degrees) (refer to the images in section 5.2.1 for more details).
fict_zero	Value considered as fictitious zero in order to avoid division by zero. NOTE: When nothing is specified in the mask, it is set to 1e-6 by default. This value usually does not need to be modified.
offset_x_ne	Defines the displacement of the North-East (NE) node from the top-right plate corner along the <i>X</i> axis. The parameter is not available when Offset_Connectivity_Point is FALSE (see table B.5). NOTE: If this parameter has a non-zero value, the following one (i.e. offset_y_ne) must be zero.
offset_y_ne	Defines the displacement of the North-East (NE) node from the top-right plate corner along the <i>Y</i> axis. The parameter is not available when Offset_Connectivity_Point is FALSE (see table B.5). NOTE: If this parameter has a non-zero value, the previous one (i.e. offset_x_ne) must be zero.
offset_z_ne	Defines the displacement of the North-East (NE) node from the top-right plate corner along the <i>Z</i> axis. The parameter is not available when Offset_Connectivity_Point is FALSE (see table B.5).
offset_x_se	Defines the displacement of the South-East (SE) node from the bottom-right plate corner along the <i>X</i> axis. The parameter is not available when Offset_Connectivity_Point is FALSE (see table B.5). NOTE: If this parameter has a non-zero value, the following one (i.e. offset_y_se) must be zero.
offset_y_se	Defines the displacement of the South-East (SE) node from the bottom-right plate corner along the <i>Y</i> axis. The parameter is not available when Offset_Connectivity_Point is FALSE (see table B.5). NOTE: If this parameter has a non-zero value, the previous one (i.e. offset_x_se) must be zero.
offset_z_se	Defines the displacement of the South-East (SE) node from the bottom-right plate corner along the <i>Z</i> axis. The parameter is not available when Offset_Connectivity_Point is FALSE (see table B.5).
offset_x_sw	Defines the displacement of the South-West (SW) node from the bottom-left plate corner along the <i>X</i> axis. The parameter is not available when Offset_Connectivity_Point is FALSE (see table B.5). NOTE: If this parameter has a non-zero value, the following one (i.e. offset_y_sw) must be zero.
offset_y_sw	Defines the displacement of the South-West (SW) node from the bottom-left plate corner along the <i>Y</i> axis. The parameter is not available when Offset_Connectivity_Point is FALSE (see table B.5). NOTE: If this parameter has a non-zero value, the previous one (i.e. offset_x_sw) must be zero.

(Continued)

Table B.6. (Continued)

Parameter	Meaning
offset_z_sw	Defines the displacement of the South-West (SW) node from the bottom-left plate corner along the Z axis. The parameter is not available when Offset_Connectivity_Point is FALSE (see table B.5).
offset_x_nw	Defines the displacement of the North-West (NW) node from the top-left plate corner along the X axis. The parameter is not available when Offset_Connectivity_Point is FALSE (see table B.5). NOTE: If this parameter has a non-zero value, the following one (i.e. offset_y_nw) must be zero.
offset_y_nw	Defines the displacement of the North-West (NW) node from the top-left plate corner along the Y axis. The parameter is not available when Offset_Connectivity_Point is FALSE (see table B.5). NOTE: If this parameter has a non-zero value, the previous one (i.e. offset_x_nw) must be zero.
offset_z_nw	Defines the displacement of the North-West (NW) node from the top-left plate corner along the Z axis. The parameter is not available when Offset_Connectivity_Point is FALSE (see table B.5).

properties window within the schematic editor. When nothing is specified (i.e. the field is left blank), its default value is set to $1e-6 \Omega$. If necessary, this value can be modified.

B.6.3 Minimum resistance block—boundary condition component

Recalling what was just discussed, a similar short circuit condition is detected by Spectre when two rigid components (i.e. rigid plates) are connected together within the same schematic. In order to avoid this issue, an element defining a minimum resistance between the input and output nodes is available within the libraries. Its subfolder name is **min_res_1_a_6_pin** and the Cadence schematic symbol is shown in figure 5.24 in the previous chapter 5. Such an element must be instanced between the two nodes of the rigid bodies to be connected together. The parameter **r_min** (minimum resistance) is accessible in the properties window within the schematic editor. When nothing is specified (i.e. the field is left blank), its default value is $1e-6 \Omega$. If necessary it can be modified. Depending on the number of nodes to be connected together, the minimum resistance element is available with different combinations other than the one in figure 5.24. The additional minimum resistance elements are available with one, two or three linear node(s), named, respectively, as **min_res_lin_1_pin**, **min_res_lin_2_pin** and **min_res_lin_3_pin**, as well as with one, two or three angular node(s), named, respectively, as **min_res_ang_1_pin**, **min_res_ang_2_pin** and **min_res_ang_3_pin**.

B.6.4 Unconnected nodes termination—boundary condition component

Given the schematic implementation corresponding to a certain RF-MEMS device to be simulated, it might happen that one or more nodes remain floating

(i.e. unconnected). This does not represent an actual issue impairing the analysis. However, in such a circumstance Spectre generates a warning message and shorts unconnected nodes to ground with a minimum conductance. In order to avoid the warning messages, a module defining an unconnected termination to which the floating nodes must be wired is available in the library. Its name within both libraries is **unc_1_a_6_pin** and the Cadence schematic symbol is shown in figure 5.25 in the previous chapter 5. Depending on the number of nodes to be terminated, the floating element is available with different combinations other than the one in figure 5.25. Such additional implementations of the unconnected nodes element are available with one, two or three linear node(s), named, respectively, as **unc_lin_1_pin**, **unc_lin_2_pin** and **unc_lin_3_pin**, as well as with one, two or three angular node(s), named, respectively, as **unc_ang_1_pin**, **unc_ang_2_pin** and **unc_ang_3_pin**.

B.6.5 Force generator—stimulus source component

This module generates a force to be applied to a certain MEMS structure. The name of the subfolder in both libraries is **force_ang_6_full_degs**. The Cadence schematic symbol is shown in figure 5.26 in the previous chapter 5. Within the Cadence schematic properties interface, four parameters are available for this component, as reported in the following table B.7.

B.6.6 Force generator (AC simulations)—stimulus source component

This module generates a force to be applied to a certain MEMS structure for small signal (AC) simulations within Spectre. Its name within both libraries is **force_ac_5_degs** and it allows only 5 DoFs (i.e. torques around the X axis cannot be imposed). Four parameters are available within the Cadence schematic properties window, as described in table B.8.

B.6.7 Force generator (pulse)—stimulus source component

The module here at stake generates a force pulse to be applied to a certain MEMS within Spectre. Its name within both libraries is **force_ang_pulse_6_degs**. Seven parameters are available within the Cadence schematic properties window, as described in table B.9.

Table B.7. Description of all the available parameters for the **force_ang_6_full_degs** model.

Parameter	Meaning
angle_y	This parameter defines the rotation (in degrees) of the force and torque (refer to the following parameters) around the Y axis.
angle_z	This parameter defines the rotation (in degrees) of the force and torque (refer to the following parameters) around the Z axis.
torque_x	This parameter defines the torque modulus ($N \cdot m$) around the X axis.
force_mod	This parameter defines the force modulus (N) to be applied.

Table B.8. Description of all the parameters available for the **force_ac_5_degs** model.

Parameter	Meaning
forza	This parameter defines the force modulus (N) to be applied.
phase	This parameter defines the phase rotation to be applied to the force.
angle_y	This parameter defines the rotation (in degrees) of the force around the <i>Y</i> axis.
angle_z	This parameter defines the rotation (in degrees) of the force around the <i>Z</i> axis.

Table B.9. Description of all the parameters available for the **force_ang_pulse_6_degs** model.

Parameter	Meaning
angle_y	This parameter defines the rotation (in degrees) of the force around the <i>Y</i> axis.
angle_z	This parameter defines the rotation (in degrees) of the force around the <i>Z</i> axis.
t_delay	This parameter defines the delay (seconds) of the pulse.
t_rise	This parameter defines the rise time (seconds) of the OFF to ON edge.
t_on	This parameter defines the duration of the pulse ON value (seconds).
t_fall	This parameter defines the fall time (seconds) of the ON to OFF edge.
force_mod	This parameter defines the force modulus (N) to be applied during the pulse ON time. The pulse low (OFF) force value is always zero.

Table B.10. Description of all the parameters available for the **displacements_ang_6_full_degs** model.

Parameter	Meaning
displacement	This parameter defines the displacement (m) to be applied to the MEMS structure.
rot_x	This parameter defines the angular rotation (degrees) to be applied to the MEMS structure around the <i>X</i> axis.
angle_y	This parameter defines the rotation (in degrees) of the linear and angular displacement around the <i>Y</i> axis.
angle_z	This parameter defines the rotation (in degrees) of the linear and angular displacement around the <i>Z</i> axis.

B.6.8 Displacement—stimulus source component

This module generates a displacement to be applied to a certain MEMS structure. The name of the model available in the libraries is **displacements_ang_6_full_degs**, while the Cadence schematic symbol is shown in figure 5.27 in the previous chapter 5. Four parameters are available in the Cadence schematic properties window, as listed in table B.10.

B.7 Conclusion

The target of this appendix was that of providing the reader with the necessary knowledge and information in order to utilise the MEMS compact model library, discussed in the previous chapter 5, concerning the mathematical models within the Cadence Integrated Circuits (ICs) development environment. The appendix was arranged as a user guide, while the software library is made available for download together with this book, and is implemented in two different Hardware Description Language (HDL)-based codes, i.e. VerilogA and SpectreHDL, within the Cadence environment (www.cadence.com), for the Spectre Circuit Simulator. The tool can be ported to other simulation environments, i.e. other than Cadence, as long as HDL codes are supported.

References

- [1] *Verilog-A—Language Reference Manual* https://siue.edu/~gengel/ece585WebStuff/OVI_VerilogA.pdf
- [2] *Affirma VerilogA Language Reference*, December, 1999 (Cadence Design Systems, Inc. Product Version 4.4.5)
- [3] *SpectreHDL Reference* December, 1999 (Cadence Design Systems, Inc. Product Version 4.4.5)
- [4] *Spectre Simulation Platform* https://cadence.com/en_US/home/tools/custom-ic-analog-rf-design/circuit-simulation/spectre-simulation-platform.html
- [5] *Affirma Spectre Circuit Simulator User Guide* June, 2000 (Cadence Design Systems, Inc. Product Version 4.4.6)
- [6] Jing Q 2003 Modeling and for design of suspended MEMS, *PhD Dissertation in Electrical and Computer Engineering* Carnegie Mellon University https://research.ece.cmu.edu/~mems/pubs/pdfs/ece/PhD_thesis/0117_jing-2003.pdf
- [7] Przemieniecki J S 1968 *Theory of Matrix Structural Analysis* (New York: McGraw-Hill)
- [8] Iannacci J 2013 *Practical Guide to RF-MEMS* 1st edn (Weinheim: Wiley) p 372
- [9] Cho Y-H, Pisano A P and Howe R T 1994 Viscous damping model for laterally oscillating microstructures *J. Microelectromech. Syst.* **3** 81–7
- [10] Veijola T, Kuisma H and Lahdenpera J 1997 Model for gas film damping in a silicon accelerometer *Proc. of the Int. Conf. on Solid-State Sensors Actuators* **4** 1097–100
- [11] Iannacci J, Gaddi R and Gnudi A 2010 Experimental validation of mixed electromechanical and electromagnetic modeling of RF-MEMS devices within a standard IC simulation environment *J. Microelectromech. Syst.* **19** 526–37